

## A comparative study of proton transport properties of zirconium phosphate and its metal exchanged phases

RAKESH THAKKAR, HEEMANSHU PATEL and UMA CHUDASAMA\*

Applied Chemistry Department, Faculty of Technology and Engineering, M.S. University of Baroda, Vadodara 390 001, India

MS received 26 December 2006; revised 7 May 2007

**Abstract.** A new phase of amorphous zirconium phosphate (ZrP), an inorganic ion exchanger of the class of tetravalent metal acid (TMA) salt, is synthesized by sol–gel method. The protons present in the structural hydroxyl groups indicate good potential for TMA salts to exhibit solid state proton conduction.  $\text{Cu}^{2+}$  and  $\text{Li}^+$  are exchanged onto ZrP to yield CuZrP and LiZrP exchanged phases. All these materials were characterized for elemental analysis (ICP–AES), thermal analysis (TGA, DSC), X-ray analysis and FTIR spectroscopy. The transport properties of these materials were explored and compared by measuring conductance at different temperatures using an impedance analyser. It is observed that conductivity decreases with increasing temperature in all cases and mechanism of transportation is proposed to be Grotthuss type. Conductivity performance of ZrP, CuZrP and LiZrP is discussed based on conductivity data and activation energy.

**Keywords.** Tetravalent metal acid salts; proton conduction; impedance analysis; proton transport properties; solid electrolytes.

### 1. Introduction

Discovering new proton conductors, and studying the mechanism of their conduction is an area of current interest, the potential use of such compounds being in fuel cells, sensors, water electrolysis units and other electrochemical devices. A brief overview on solid state proton conductors has been reported in literature (Norby 1999; Alberti and Casciola 2001; Hogarth *et al* 2005).

Proton conductors are often considered to be electrolytes in which hydrogen is transported towards the cathode during electrolysis. Proton transport includes transport of proton ( $\text{H}^+$ ) and any assembly that carries protons ( $\text{OH}^-$ ,  $\text{H}_2\text{O}$ ,  $\text{H}_3\text{O}^+$ ,  $\text{NH}_4^+$ ,  $\text{HS}^-$ , etc) (Grotthuss 1806). The transport of protons ( $\text{H}^+$ ) between relatively stationary host anions has been termed the ‘Grotthuss’ or ‘free-proton’ mechanism. The Grotthuss mechanism requires close proximity of water molecules, which are firmly held but able to rotate. Transport by any other species is termed as ‘vehicle mechanism’. Vehicle mechanism is most frequently encountered in aqueous solution and other liquid/melts. In solids, vehicle mechanism is usually restricted to materials with open structures (channels, layers) to allow passage of the large ions and molecules. Compounds with less amount of water would be expected to conduct by vehicle mechanism in which a nucleophilic group such as  $\text{H}_2\text{O}$  or

$\text{NH}_3$  acts as a proton carrier. The classification of proton conductors according to the preparation method, chemical composition, structural dimensionality, mechanism of conduction, etc has been summarized in a comprehensive book on proton conductors (Ikawa 1992).

Inorganic cation exchangers of the class of tetravalent metal acid (TMA) salts exhibit the general formula,  $\text{M}(\text{IV})(\text{HXO}_4)_2 \cdot n\text{H}_2\text{O}$ , where  $\text{M}(\text{IV}) = \text{Zr}, \text{Ti}, \text{Sn}, \text{Ce}, \text{Th}$  etc and  $\text{X} = \text{P}, \text{Mo}, \text{W}, \text{As}, \text{Sb}$  etc. The number of water molecules depends on the method of preparation and drying conditions. TMA salts possess structural hydroxyl protons, which are responsible for their ion exchange behaviour. The protons present in the structural hydroxyl groups indicate good potential for TMA salts to exhibit solid state proton conduction. When these  $-\text{OH}$  groups are hydrated, the protons can move easily on the surface, thus accounting for their conductivities, which depend strongly on relative humidity, the surface area and the degree of crystallinity (Clearfield and Berman 1981). Alberti and coworkers have shown that the surface conducts protons thousand times faster than the bulk protons (Alberti *et al* 1978).

The mechanism of diffusion and proton transport in crystalline zirconium phosphate and titanium phosphate has been studied in detail by various workers (Alberti 1976; Alberti *et al* 1978, 1979; Howe and Shelton 1979; Yamanaka 1980; Clearfield and Jerus 1982; Boilot *et al* 2003). An earlier investigation on zirconium phosphate with varying degrees of crystallinity showed that the conducti-

\*Author for correspondence (uvrcres@gmail.com)

vity decreased considerably with increasing degree of crystallinity (Hamlem 1962; Alberti and Torracca 1968; Alberti *et al* 1978).

From our laboratory, we have reported proton transport properties in amorphous zirconium phosphomolybdate and its single salt counterparts viz. zirconium molybdate and zirconium phosphate (Beena and Chudasama 1996) and of M(IV) tungstates (Parikh and Chudasama 2003), where M(IV) = Sn, Ti, Zr. Szirtes and coworkers reported the conductivity of transition metal exchanged phases of crystalline zirconium phosphate (Szirtes *et al* 2001) and titanium phosphate (Szirtes *et al* 2003). Ramos-Barrado and coworkers reported the conductivity of Li<sup>+</sup> exchanged layered tin phosphate materials (Ramos-Barrado *et al* 1994) and Li<sup>+</sup> exchanged pillared *a*-zirconium phosphate (Ramos-Barrado *et al* 1997).

Literature survey reveals that not much work has been done on the transport properties of amorphous zirconium phosphate and its metal exchanged phases. In the present endeavour, amorphous zirconium phosphate (ZrP) was synthesized by sol-gel method. Cu<sup>2+</sup> and Li<sup>+</sup> are exchanged onto ZrP to yield CuZrP and LiZrP exchanged phases. All these materials were characterized for elemental analysis (ICP-AES), thermal analysis (TGA, DSC), X-ray analysis and FTIR spectroscopy. Chemical resistivity was assessed in acids, bases and organic solvent media. The transport properties of these materials were explored by measuring conductance at different temperatures in the range 30–120°C at 10°C intervals, using SOLARTRON DATASET impedance analyser (SI 1260) over a frequency range 1 Hz–10 MHz at a signal level below 1 V. Based on the conductance data and Arrhenius plots, a suitable mechanism is proposed, and conductance performance of ZrP, CuZrP and LiZrP compared.

## 2. Experimental

### 2.1 Preparation of ZrP and metal exchanged phases (CuZrP and LiZrP)

ZrP was prepared by mixing aqueous solutions of ZrOCl<sub>2</sub>·8H<sub>2</sub>O (0.1 M, 100 ml) and sodium dihydrogen phosphate (0.2 M, 100 ml) in the pH range 1–2, drop by drop and with continuous stirring at 70°C. The gelatinous precipitate obtained was digested for an hour at 70°C, filtered and washed with conductivity water till removal of chloride ions, followed by drying at room temperature.

The material was sized by sieving [30–60 mesh (ASTM)] and finally converted to acid form by treating 5 g of the material with 50 ml of 1 M HNO<sub>3</sub> for 30 min with occasional shaking. The sample was then separated from acid by decantation and washed with double distilled water for removal of adhering acid. This process (acid treatment) was repeated at least five times. After final washing, the material was dried at room temperature.

CuZrP and LiZrP were prepared by equilibrating 2 g ZrP with 200 ml of 0.2 M copper acetate or lithium acetate solution as the case may be, with continuous stirring at 50°C for 100 h. The solid was separated by filtration and washed with conductivity water for removal of adhering ions and dried at room temperature.

### 2.2 Instrumentation

The samples were analysed for zirconium, copper, lithium and phosphorous contents by ICP-AES. X-ray diffractograms ( $2\theta = 5\text{--}80^\circ$ ) were obtained on X-ray diffractometer (Rigaku Dmax 2200) with Cu-K $\alpha$  radiation and nickel filter. FTIR spectra were recorded using KBr wafer on a Bomem MB series. Thermal analyses (TGA, DSC) were carried out on a Shimadzu thermal analyser at a heating rate of 10°C/min. Chemical resistivity in various media (acids, bases and organic solvents) was studied by taking 500 mg of ZrP in 50 ml of the particular medium and allowing to stand for 24 h. The change in colour, nature and weight was observed. The Na<sup>+</sup> ion exchange capacity (IEC) of ZrP was determined by column method (Nabi and Rao 1981). Further, the effect of heating on IEC was studied by heating several 1 g portions of the exchangers for 2 h in the temperature range 100–500°C at an interval of 100°C in a muffle furnace and determining the Na<sup>+</sup> exchange capacity by the column method (Nabi and Rao 1981) at room temperature.

### 2.3 Conductivity measurements

The conductivity of the materials was measured on pellets of 10 mm diameter and 1.5–2 mm thickness. The opposite sides of the pellets were coated with conducting silver paste to ensure good ohmic contact. Complex impedance was measured in the temperature range 30–120°C, at 10°C intervals using SOLARTRON DATASET impedance analyser (SI 1260), over a frequency range 1 Hz–10 MHz at a signal level below 1 V, interfaced to a minicomputer for data collection. In all cases, since the impedance plots of the materials consist of single depressed semicircle, the conductivity was obtained by arc extrapolation to the real axis, taking into account the geometrical sizes of the pellets.

## 3. Results and discussion

### 3.1 Characterization

ZrP was obtained as white hard granules, while LiZrP and CuZrP were obtained as white and blue powders, respectively. Elemental analysis carried out using ICP-AES showed the ratio of Zr:P in ZrP, CuZrP and LiZrP to be 1:2. For all characterizations (X-ray, FTIR, thermal), as

a representative, figures of ZrP are presented since all three materials exhibit almost similar behaviour. The absence of any sharp peaks in the X-ray powder diffractograms (figure 1) for ZrP, CuZrP and LiZrP indicates the amorphous nature of the materials.

The FTIR spectra of ZrP (figure 2) exhibits a broad band in the region  $\sim 3400\text{ cm}^{-1}$  which is attributed to asymmetric and symmetric  $-\text{OH}$  stretching. A sharp medium band at  $1635\text{ cm}^{-1}$  is attributed to aquo ( $\text{H}-\text{O}-\text{H}$ ) bending. A band in the region  $\sim 1035\text{ cm}^{-1}$  is attributed to the presence of  $\text{P}=\text{O}$  stretching. A medium intensity band at  $1400\text{ cm}^{-1}$  is attributed to the presence of  $\delta(\text{POH})$  (Slade *et al* 1997). These bands indicate the presence of structural hydroxyl groups/protonic sites in the material. There is no drastic change observed in band position in the FTIR spectrum of CuZrP and LiZrP as compared to ZrP. However, metal-oxygen stretches i.e.  $\text{Cu}-\text{O}$  and  $\text{Li}-\text{O}$ , have been obtained at  $627\text{ cm}^{-1}$  and  $526\text{ cm}^{-1}$ , respectively (Robinson 1974), confirming the formation of CuZrP and LiZrP. The  $\text{Na}^+$  exchange capacity of ZrP, evaluated at room temperature, is  $2.77\text{ meq g}^{-1}$ . The effect of calcination on IEC studied in the temperature range  $100\text{--}500^\circ\text{C}$  at an interval of  $100^\circ\text{C}$  is 2.82, 2.55, 2.39, 1.69 and  $1.46\text{ meq g}^{-1}$ , respectively. In general, it is observed that IEC decreases with increasing temperature. A drastic decrease in IEC beyond  $300^\circ\text{C}$  is attributed to condensation of structural hydroxyl groups.

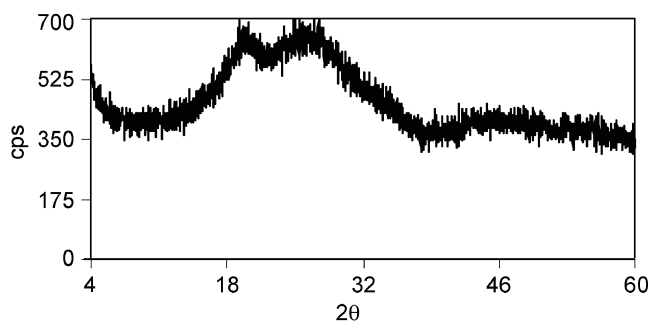


Figure 1. XRD pattern for ZrP.

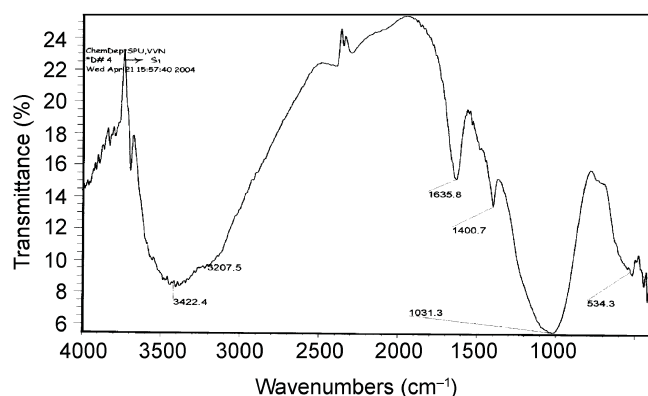


Figure 2. FTIR spectra of ZrP.

Thermal behaviour of several TMA salts have been investigated and generally examined for loss of moisture,  $\sim 80^\circ\text{C}$ , loss of external water molecules,  $\sim 100\text{--}180^\circ\text{C}$  and  $\sim 180\text{--}400^\circ\text{C}$  and above, for condensation of the structural hydroxyl groups (the H of the OH being exchange sites for cation exchanger, herein). TGA of ZrP (figure 3) shows gradual weight loss. This is explained in terms of two weight loss regions. The first weight loss,  $\sim 13\%$  up to  $180^\circ\text{C}$ , is attributed to loss of moisture/hydrated water. The second weight loss,  $\sim 2.5\%$  in the range  $250\text{--}500^\circ\text{C}$ , is attributed to condensation of structural hydroxyl groups. The DSC curve of ZrP (figure 4) exhibits an endothermic peak ( $\sim 100^\circ\text{C}$ ), which may be attributed to loss of moisture/hydrated water. An endothermic process which starts at  $\sim 300^\circ\text{C}$  could be attributed to the condensation of structural hydroxyl groups. These observations are further supported by the fact that IEC decreases on calcination, as discussed above.

Based on the elemental analysis (ICP-AES) and thermal analysis (TGA) data, ZrP, CuZrP and LiZrP, are formulated as  $\text{Zr}(\text{HPO}_4)_2 \cdot 2.5\text{H}_2\text{O}$ ,  $\text{ZrCu}_{0.18}\text{H}_{1.82}(\text{PO}_4)_2 \cdot 2.5\text{H}_2\text{O}$  and  $\text{ZrLi}_{0.6}\text{H}_{1.4}(\text{PO}_4)_2 \cdot 2.5\text{H}_2\text{O}$ , respectively. The number of water molecules in each case was calculated using Alberti and Torracca (1968) formula.

ZrP is found to be stable in acid medium, maximum tolerable limits being 36 N  $\text{H}_2\text{SO}_4$ , 16 N  $\text{HNO}_3$ , 10 N  $\text{HCl}$  and also stable in organic solvent media (ethanol, benzene,

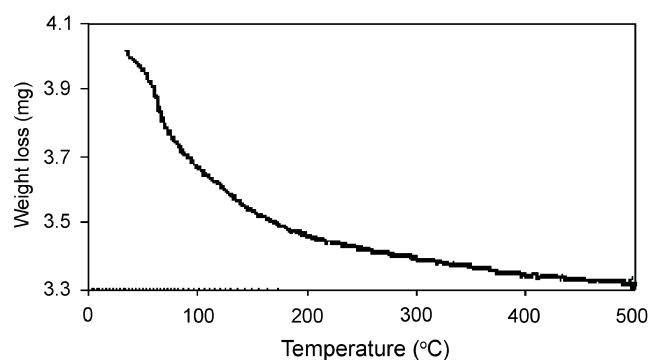


Figure 3. TGA plot for ZrP.

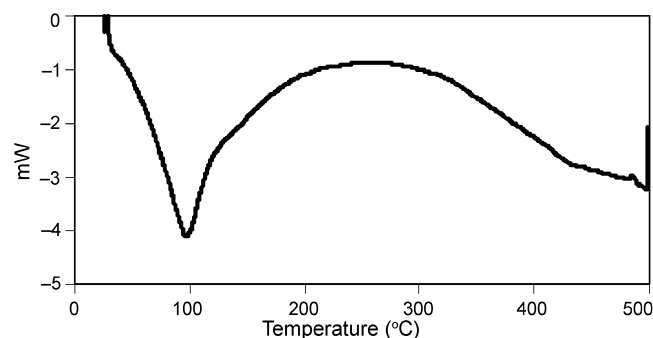


Figure 4. DSC curve for ZrP.

acetone and acetic acid) but not so stable in base medium, maximum tolerable limits being 5 N NaOH and 5 N KOH.

### 3.2 Impedance measurements

Conductivity measured in the range 30–120°C for ZrP as well as its metal exchanged phases is presented in table 1. Since the complex impedance plots of ZrP, CuZrP and LiZrP are similar (semicircular in nature), as a representative, the impedance plot of ZrP (at 30°C) is presented in figure 5.

In case of ZrP, it is observed that conductivity decreases with increasing temperature (table 1). This is attributed to the loss of water of hydration as well as condensation of structural hydroxyl groups with increasing temperature. This fact is also supported by the study of effect of heating on IEC as discussed above. This suggests the mechanism of transportation to be of Grotthuss type (Clearfield 1988) where the conductivity depends on the ability of water located on the surface to rotate and participate. Further, the results are also in agreement with the suggestion that protons are not able to diffuse along an anhydrous surface where the spacing of the –OH groups is too high (Alberti *et al* 1989). Besides, the fact that the loss of protons resulting from hydroxyl condensation causes a considerable

decrease in conductivity, indicating that the conduction is protonic also. In the present study, the conductivity of ZrP at 30°C is  $4.2 \times 10^{-6} \text{ Scm}^{-1}$ . Similar values have been reported for  $\alpha$ -ZrP ( $3.2 \times 10^{-6} \text{ Scm}^{-1}$ ) (Casciola and Bianchi 1985) and polymer electrolyte blends (Paulmer and Kulkarni 1992; Subramony and Kulkarni 1994; De *et al* 2005). The values are, however, lower by two orders of magnitude compared to modified forms like pellicular ZrP ( $1.1 \times 10^{-4} \text{ Scm}^{-1}$ ) (Casciola and Costantino 1986).

In the present study, the conductivity of CuZrP ( $8.5 \times 10^{-7} \text{ Scm}^{-1}$ ) is about one order of magnitude lower compared to ZrP ( $4.2 \times 10^{-6} \text{ Scm}^{-1}$ ). Similar studies carried out by Szirtes and coworkers on transition metal exchanged phases of crystalline ZrP (Szirtes *et al* 2001) show that in case of  $\text{Cu}^{2+}$  exchanged phases, the conductivity,  $5.8 \times 10^{-6} \text{ Scm}^{-1}$ , has been an order of magnitude lower compared to the parent ZrP ( $2.85 \times 10^{-5} \text{ Scm}^{-1}$ ).

In case of LiZrP, the conductivity at 30°C is  $7.8 \times 10^{-6} \text{ Scm}^{-1}$ . The conductivity decreases with increasing temperature up to 120°C and then increases at higher temperatures. At a temperature as high as 250°C the conductivity value is of the order of  $5.1 \times 10^{-6} \text{ Scm}^{-1}$ . Complex impedance plot of LiZrP at 200°C exhibits a semicircular behaviour. The conductance values remain constant ( $\sim 10^{-6}$ ) in the temperature range 30–250°C. At higher temperatures, ZrP itself starts giving disordered complex

**Table 1.** Conductivity ( $\text{Scm}^{-1}$ ) of ZrP, CuZrP and LiZrP.

Temperature (°C)	Conductivity, $\sigma$ ( $\text{Scm}^{-1}$ )		
	$\sigma_{\text{ZrP}}$	$\sigma_{\text{CuZrP}}$	$\sigma_{\text{LiZrP}}$
30	$4.20 \times 10^{-6}$	$8.50 \times 10^{-7}$	$7.80 \times 10^{-6}$
40	$3.80 \times 10^{-6}$	$7.20 \times 10^{-7}$	$4.20 \times 10^{-6}$
50	$3.50 \times 10^{-6}$	$6.40 \times 10^{-7}$	$3.20 \times 10^{-6}$
60	$3.10 \times 10^{-6}$	$5.10 \times 10^{-7}$	$3.12 \times 10^{-6}$
70	$2.80 \times 10^{-6}$	$3.20 \times 10^{-7}$	$3.01 \times 10^{-6}$
80	$2.80 \times 10^{-6}$	$1.06 \times 10^{-7}$	$2.60 \times 10^{-6}$
90	$2.60 \times 10^{-6}$	$8.40 \times 10^{-8}$	$2.60 \times 10^{-6}$
100	$2.30 \times 10^{-6}$	$6.04 \times 10^{-8}$	$2.40 \times 10^{-6}$
110	$2.10 \times 10^{-6}$	$3.02 \times 10^{-8}$	$2.25 \times 10^{-6}$
120	$1.90 \times 10^{-6}$	$1.80 \times 10^{-8}$	$2.12 \times 10^{-6}$
200	–	–	$4.50 \times 10^{-6}$
250	–	–	$5.10 \times 10^{-6}$
$E_{\text{act}}$ (kcal/mol)	1.00	13.80	0.51

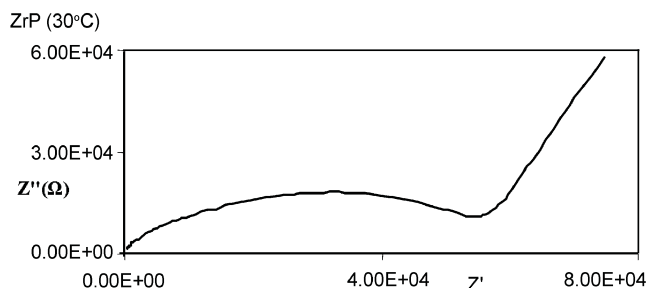


**Figure 5.** Complex impedance plot for ZrP at 30°C.

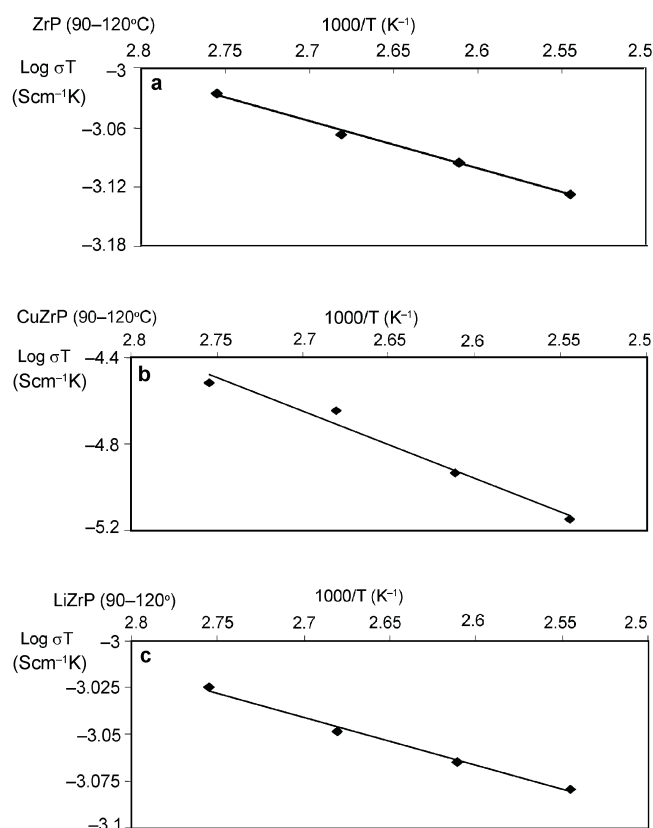


**Figure 6.** Arrhenius plot for (a) ZrP, (b) CuZrP and (c) LiZrP in the range 90–120°C.

impedance plots. The conduction behaviour observed in case of LiZrP, in the present study, is similar to that of other Li<sup>+</sup> exchanged materials. Ramos-Barrado *et al* (1994, 1997) and Criado *et al* (1993) have explained this to be due to the contribution of two types of charge carriers. The first one is a low temperature conduction, due to proton mobility, that depends on the zeolitic water content, and decreases with increasing temperature. The second, a high temperature conduction, is due to the mobility of Li<sup>+</sup>, which increases with increasing temperature, giving rise to an increase in the net conductivity. Unusually high conductivity at elevated temperatures is also reported in lithium oxyfluorophosphate system [LiF–Li<sub>2</sub>O–Al(PO<sub>3</sub>)<sub>3</sub>] (Evastrop'ev *et al* 1974; Jagla and Isard 1980; Maiti *et al* 1983). Yamanaka (1980) studied the conduction behaviour of *a*-ZrP and its alkali metal exchanged phases and observed the order to be,  $E_{act}, K^+ > Na^+ > Li^+ > H^+$  and explained it to be correlated to the increase in ionic radius of the exchanged alkali metal ion. The diffusion of the cations and hence conductance becomes difficult with an increase in the cationic radius. Similar trend has also been observed by Alberti and coworkers for  $\gamma$ -titanium phosphate and its alkali metal exchanged phases (Alberti *et al* 1982) as well as ZrP alkali metal exchanged phases (Alberti *et al* 1979; Yamanaka 1980; Clearfield and Jerus 1982).

Arrhenius plots are presented in figures 6a–c. For all the three materials linearity is observed in the temperature range 90–120°C. The energy of activation ( $E_{act}$ , kcal/mol) values observed are 13.80 (CuZrP), 0.51 (LiZrP) and 1.00 (ZrP). Almost similar values of  $E_{act}$  for LiZrP and ZrP could be attributed to almost same order of magnitude of conductance in the range 90–120°C. The  $E_{act}$  trend observed for exchanged phases of CuZrP > LiZrP could be attributed to hindrance to the diffusion of the cation and hence conductance with increasing size of cation, which plays a significant role.

#### 4. Conclusion

In the present study, it is observed that lithium exchanged phase exhibits encouraging transport properties which are also comparable to literature reports.

#### Acknowledgements

The authors acknowledge UGC, New Delhi, for financial assistance and the help rendered by Prof. A R Kulkarni, Indian Institute of Technology, Mumbai, in impedance measurements.

#### References

Alberti G 1976 *Study week on biological and artificial membranes and desalination of water* (ed.) R Passino (Vatican City: Varia, Pontificia Academia Scientiarum Scripta) p. 629

- Alberti G and Torracca E 1968 *J. Inorg. Nucl. Chem.* **30** 1093, 3075
- Alberti G and Casciola M 2001 *Solid State Ionics* **145** 3
- Alberti G, Casciola M, Costantino U, Levi G and Riccardi G 1978 *J. Inorg. Nucl. Chem.* **40** 533
- Alberti G, Casciola M, Costantino U and Radi G 1979 *Gazz. Chim. Ital.* **109** 421
- Alberti G, Bracardi M and Casciola M 1982 *Solid State Ionics* **7** 243
- Alberti G, Costantino U and Polambari R 1989 *First international conference on inorganic membranes, Montpellier, France*, p. 25
- Beena B and Chudasama U 1996 *Bull. Mater. Sci.* **19** 405
- Boilot J P, Barboux P, Carrier D, Lhalil K and Moreau M 2003 *Solid State Ionics* **162–163** 185
- Casciola M and Costantino U 1986 *Solid State Ionics* **20** 69
- Casciola M and Bianchi D 1985 *Solid State Ionics* **17** 287
- Clearfield A 1988 *J. Mol. Catal.* **88** 125
- Clearfield A and Berman J R 1981 *J. Inorg. Nucl. Chem.* **43** 2141
- Clearfield A and Jerus P 1982 *Solid State Ionics* **6** 79
- Criado C, Ramos-Barrado J R, Maireles-Torres P, Olivera-Pastor P, Rodriguez-Castellon E and Jimenez-Lopez A 1993 *Solid State Ionics* **61** 139
- De S, De A, Das A and De S K 2005 *Mater. Chem. & Phys.* **91** 477
- Evastrop'ev K K, Veksler G I and Kondrat'eva B S 1974 *Dokl. Akad. Nauk. SSSR* **215** 902
- Grothuss C J D 1806 *Ann. Chim.* **58** 54
- Hamlem R P 1962 *J. Electrochem. Soc.* **109** 746
- Hogarth W H J, Diniz da Costa J C and Lu (Max) G Q 2005 *J. Power Sources* **142** 223
- Howe A T and Shelton M G 1979 *J. Solid State Chem.* **28** 345
- Ikawa H 1992 *Proton conductors* (ed.) P Colomban (New York: Cambridge University Press) p. 190
- Jagla M and Isard J Q 1980 *Mater. Res. Bull.* **15** 1327
- Maiti H S, Kulkarni A R and Paul A 1983 *Solid State Ionics* **9/10** 605
- Nabi S A and Rao R K 1981 *J. Indian Chem. Soc.* **11** 1030
- Norby T 1999 *Solid State Ionics* **125** 1
- Parikh A and Chudasama U 2003 *Proc. Indian Acad. Sci. (Chem. Sci.)* **115** 1
- Paulmer R D A and Kulkarni A R 1992 *Solid state ionics: Materials and applications* (ed.) B V R Chowdari (Singapore: World Scientific) p. 549
- Ramos-Barrado J R, Criado C, Maireles-Torres P, Olivera-Pastor P, Rodriguez-Castellon E and Jimenez-Lopez A 1994 *Solid State Ionics* **73** 67
- Ramos-Barrado J R, Martin F, Rodriguez-Castellon E, Jimenez-Lopez A, Olivera-Pastor P and Perez-Reina F 1997 *Solid State Ionics* **97** 187
- Robinson J W 1974 *Handbook of spectroscopy* (Ohio: CRC press) **Vol. 2**, p. 99
- Slade R C T, Knowles J A, Jones D J and Roziere J 1997 *Solid State Ionics* **96** 9
- Subramony J A and Kulkarni A R 1994 *Mater. Sci. & Engg.* **B22** 206
- Szirtes L, Kuzmann E, Megyeri J and Klencsar Z 2001 *Solid State Ionics* **145** 257
- Szirtes L, Megyeri J, Riess L and Kuzmann E 2003 *Solid State Ionics* **162–163** 181
- Yamanaka S 1980 *J. Inorg. Nucl. Chem.* **24** 717